

# PB1 Domain-Mediated Heterodimerization in NADPH Oxidase and Signaling Complexes of Atypical Protein Kinase C with Par6 and p62

Michael I. Wilson,<sup>1</sup> David J. Gill,<sup>1</sup> Olga Perisic,<sup>1</sup>  
Mark T. Quinn,<sup>2</sup> and Roger L. Williams<sup>1,\*</sup>

<sup>1</sup>MRC Laboratory of Molecular Biology  
Hills Road  
Cambridge CB2 2QH  
United Kingdom

<sup>2</sup>Veterinary Molecular Biology  
Montana State University  
Bozeman, Montana 59717

## Summary

**Maximal activation of NADPH oxidase requires formation of a complex between the p40<sup>phox</sup> and p67<sup>phox</sup> subunits via association of their PB1 domains. We have determined the crystal structure of the p40<sup>phox</sup>/p67<sup>phox</sup> PB1 heterodimer, which reveals that both domains have a  $\beta$  grasp topology and that they bind in a front-to-back arrangement through conserved electrostatic interactions between an acidic OPCA motif on p40<sup>phox</sup> and basic residues in p67<sup>phox</sup>. The structure enabled us to identify residues critical for heterodimerization among other members of the PB1 domain family, including the atypical protein kinase C $\zeta$  (PKC $\zeta$ ) and its partners Par6 and p62 (ZIP, sequestosome). Both Par6 and p62 use their basic “back” to interact with the OPCA motif on the “front” of the PKC $\zeta$ . Besides heterodimeric interactions, some PB1 domains, like the p62 PB1, can make homotypic front-to-back arrays.**

## Introduction

Professional phagocytes such as neutrophils and macrophages are key components of the innate immune system. These cells rapidly engulf and destroy microbes. One of the early events in this process is production of superoxide (O<sub>2</sub><sup>-</sup>) by activated NADPH oxidase (Babior, 1999). The importance of the oxidase is apparent from life-threatening and recurring infections that occur in individuals with chronic granulomatous disease (CGD) due to hereditary mutations in the proteins forming the NADPH oxidase complex. Because of the potential damage that can be caused by the reactive oxygen species produced by NADPH oxidase catalysis, it is tightly regulated. The catalytic machinery of the enzyme that reduces molecular oxygen, the flavocytochrome b<sub>558</sub>, consists of two intrinsic membrane subunits, p22<sup>phox</sup> and gp91<sup>phox</sup>. The flavocytochrome b<sub>558</sub> is activated by a complex of cytosolic regulatory subunits consisting of p40<sup>phox</sup>, p47<sup>phox</sup>, p67<sup>phox</sup>, and the GTPase Rac. Although cytosolic p47<sup>phox</sup>, p40<sup>phox</sup>, and p67<sup>phox</sup> subunits form a stable heterotrimeric complex in vitro (Lapouge et al., 2002), recent studies of polymorphonuclear leukocytes suggest that in the resting state p40<sup>phox</sup> and p67<sup>phox</sup> associate as a heterodimer and that the p47<sup>phox</sup>-containing heterotrimer forms only upon cell activation (Brown et

al, 2003). The molecular organization of these cytosolic regulatory subunits has been the subject of several recent structural investigations; however, much remains unexplained (Lapouge et al., 2000; Bravo et al., 2001; Grizot et al., 2001a; Hiroaki et al., 2001; Kami et al., 2002; Karathanassis et al., 2002).

Two high-affinity protein/protein interactions within the heterotrimeric complex are essential for its stability. The p67<sup>phox</sup> interacts with the p47<sup>phox</sup> subunit via its C-terminal SH3 domain (Kami et al., 2002), while the p40<sup>phox</sup> and p67<sup>phox</sup> interact through their PB1 modules (Nakamura et al., 1998). The interaction between p40<sup>phox</sup> and p67<sup>phox</sup> via the PB1 domains leads to enhanced membrane translocation of p47<sup>phox</sup> and p67<sup>phox</sup> subunits in stimulated cells, resulting in increased NADPH oxidase activity (Kuribayashi et al., 2002).

The region between the two SH3 domains in p67<sup>phox</sup> was originally referred to as the PB1 domain for its occurrence in phagocyte oxidase and Bem1p, whereas the C-terminal region from p40<sup>phox</sup> has been referred to as a PC domain for its occurrence in phagocyte oxidase and cdc24 (Ponting, 1996; Nakamura et al., 1998; Ito et al., 2001; Terasawa et al., 2001). However, recent sequence analysis has suggested that these domains should be classified as a single family known as PB1 domains and that the PC/PB1 interaction is actually a PB1 domain heterodimerization (Ponting et al., 2002). We have adopted this unifying PB1 nomenclature. Similarly, we have adopted the suggested name “OPCA-motif” for the short sequence motif present in some PB1 domains, that previously has been referred to as the octicosapeptide repeat (OPR), PC motif (phox and cdc24p), and the AID motif (atypical protein kinase C-interaction domain). It is important to note that the OPCA motif is not synonymous with a PB1 domain. The OPCA motif is present only in a subset of PB1 domains and, as we show here, this motif needs to be present only in one partner of a PB1 domain heterodimer.

The PB1 domains are present in 29 proteins in the human genome, including p40<sup>phox</sup>, p67<sup>phox</sup>, atypical protein kinases (PKC $\lambda$ , PKC $\zeta$ ), the adaptor proteins Par6 and p62 (ZIP, sequestosome 1, A170), MAPK kinase (MEK5 or MAPKK5), and MAPK kinase kinases (MEKK2 and MEKK3) (Figure 1A) (Ponting et al., 2002). PB1 family members are capable of forming specific heterodimers that are essential for the function of protein complexes such as Bem1/cdc24, p40<sup>phox</sup>/p67<sup>phox</sup>, PKC $\zeta$ /Par6, PKC $\zeta$ /p62, PKC $\zeta$ /MEK5, and MEK5/MEKK2 (Moscat and Diaz-Meco, 2000; Ito et al., 2001; Sun et al., 2001; Terasawa et al., 2001). The PB1 domain-mediated PKC $\zeta$ /Par6 polarity complex triggers phosphorylation and regulation of downstream target proteins such as GSK-3 $\beta$  (Etienne-Manneville and Hall, 2003a) and Lgl (Plant et al., 2003) that control cell polarity. Heterodimerization of PKC $\zeta$  with adaptor protein p62 (ZIP) links PKC $\zeta$  to target proteins such as the Kv $\beta$ 2 subunit of the voltage-gated potassium channel (Gong et al., 1999), the  $\rho$  subunit of GABA<sub>C</sub> receptor (Crocì et al., 2003), and scaffolding protein RIP involved in NF- $\kappa$ B activation (Sanz et al., 1999). The PB1 domain of the TRK-T3 oncoprotein has

\*Correspondence: rlw@mrc-lmb.cam.ac.uk

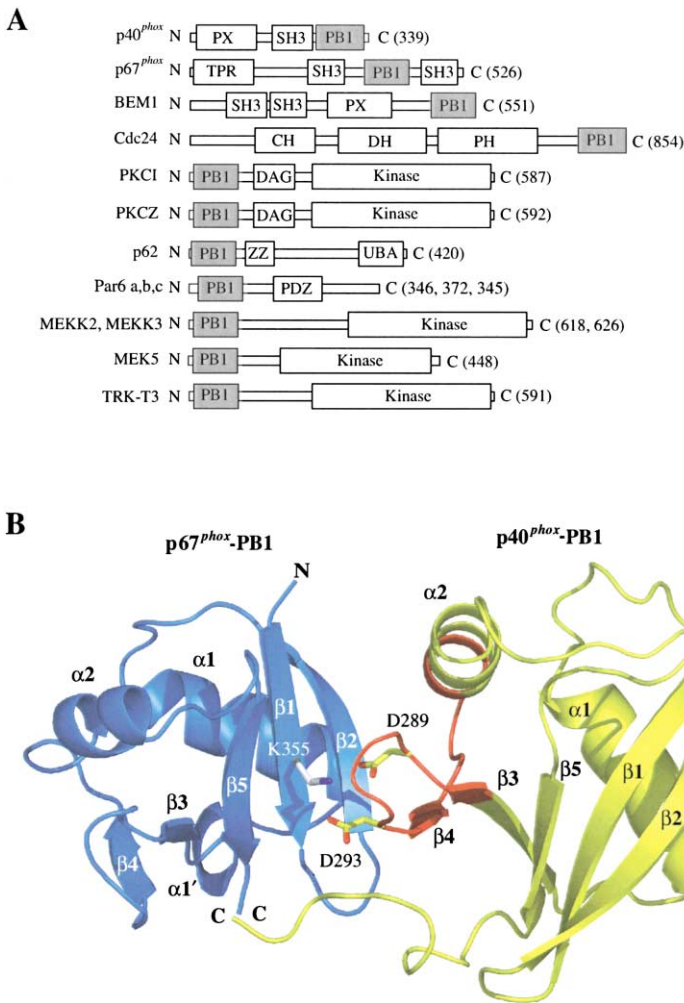


Figure 1. Many Proteins Use the PB1 Domain for Heterodimerization Including p40<sup>phox</sup> and p67<sup>phox</sup>

(A) A block diagram of the domain organization of several PB1-containing proteins (according to Pfam [Bateman et al., 2000]). The other domains present in these proteins are phagocyte oxidase, PX; Src homology 3, SH3; calponin homology, CH; Dbl/RhoGEF homology, DH; pleckstrin homology, PH; diacylglycerol/phorbol ester binding domain, DAG; serine/threonine protein kinase, Kinase; zinc finger, ZZ; ubiquitin associated, UBA; and tetratricopeptide repeat, TPR. The numbers of residues present in each protein is indicated in parentheses.

(B) A schematic representation of the p40<sup>phox</sup> PB1/p67<sup>phox</sup> PB1 heterodimer. The p67<sup>phox</sup> PB1 is rendered as a blue ribbon, and the p40<sup>phox</sup> PB1 is shown in yellow. The p40<sup>phox</sup> PB1 OPCA motif is highlighted in red. The central D289<sup>p40</sup>, D293<sup>p40</sup>/K355<sup>p67</sup> electrostatic interaction that is critical to heterodimer formation is shown in stick representation.

an indispensable role in TRK-T3 oncogenic activity (Roccatto et al., 2003).

To understand the molecular architecture of the PB1 family of heterodimers, we have determined the 2.0 Å resolution X-ray crystallographic structure of the complex of the PB1 domains from p40<sup>phox</sup> and p67<sup>phox</sup>. From this structure it is clear how PB1 domains interact with each other in a front-to-back fashion to make heterodimers and in some cases longer arrays. We have established the critical determinants of the PKCζ heterodimerization with two of its signaling partners, Par6 and p62, and demonstrated that the p62 PB1 domain is capable of forming front-to-back homoarrays.

## Results and Discussion

### Overall Fold of the Heterodimer

The complex of the PB1 domains from p40<sup>phox</sup> and p67<sup>phox</sup> crystallized in space group P6<sub>3</sub> with unit cell dimensions a = 151.4 Å, c = 68.3 Å and four heterodimers per asymmetric unit (Figure 1B). The heterodimer consists of residues 237–339 of the human p40<sup>phox</sup> and residues 352–429 of human p67<sup>phox</sup>. Both PB1 domains in the heterodimer have the same topology, an ubiquitin-like, β grasp fold, and they closely superimpose (Figures 2A and 2B). The domain consists of two α helices and a

mixed five-stranded β sheet with a 2-1-5-3-4 strand order. The sheet has a curved face that grasps helix α1. A wide splay between the N-terminal end of strand β5 and the C-terminal end of strand β3 provides a space into which helix α2 fits. The domains have a hydrophobic core between the β sheet and the hydrophobic faces of the amphipathic α helices. A convex surface formed by strand β2 of the p67<sup>phox</sup> PB1 fits into the concave surface of the p40<sup>phox</sup> PB1 formed by helix α2 resting against the surface of strands β3 and β4. Strands β2 of the p67<sup>phox</sup> PB1 and β4 of the p40<sup>phox</sup> meet at the heterodimer interface where they run approximately perpendicular to each other.

### Structure of the Heterodimeric Interface

The two PB1 domains in the complex form a front-to-back interaction with each other so that different regions of the two topologically equivalent PB1 domains make up the interface. The two interacting surfaces have a distinct electrostatic polarity. The back of the p67<sup>phox</sup> PB1 is basic, while the front of the p40<sup>phox</sup> PB1 with which it interacts is acidic (Figures 3A and 3B). The “back” of p67<sup>phox</sup> consisting of residues in strands β1 and β2 and the C-terminal end of helix α1 forms a convex surface that interlocks with a concave surface on the

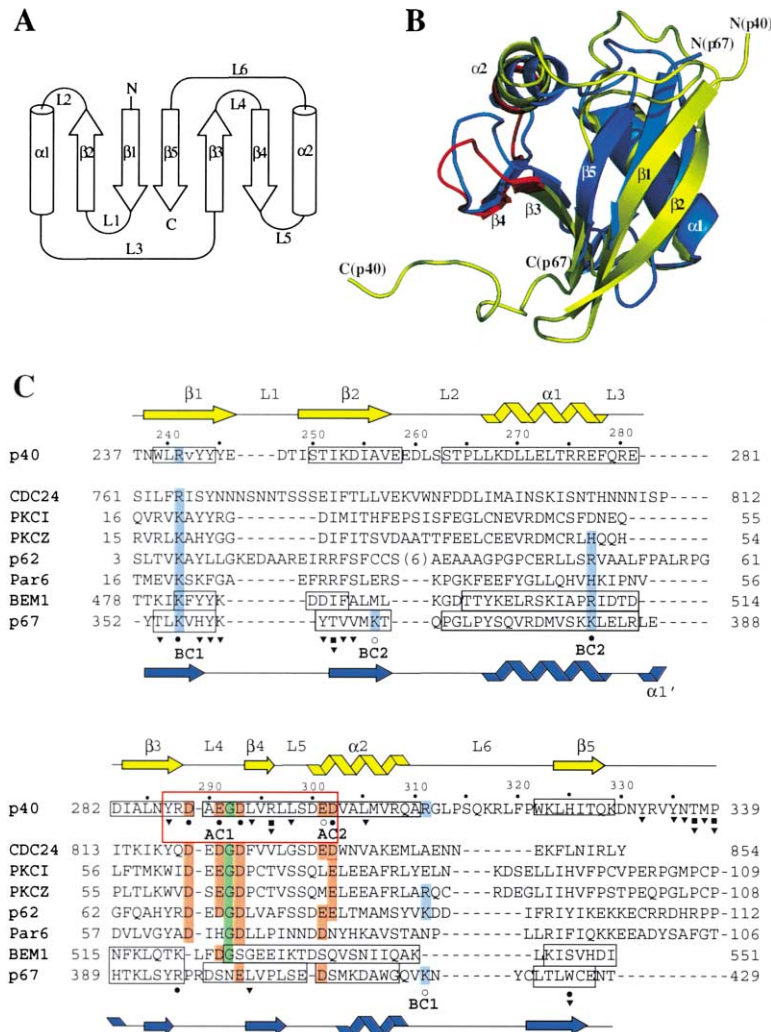


Figure 2. Structural Similarity between the p40<sup>phox</sup> and p67<sup>phox</sup> PB1 Domains and Comparison with Other PB1 Sequences

(A) The schematic topology diagram of the p40<sup>phox</sup> and p67<sup>phox</sup> PB1 domains showing an ubiquitin-like fold (the short α1' helix, which is present only in p67<sup>phox</sup>, is omitted in the diagram).

(B) A superposition (rmsd 1.6 Å) of the p40<sup>phox</sup> and p67<sup>phox</sup> PB1 domains colored as in Figure 1.

(C) A comparison of PB1 sequences based on the alignment from SMART and corrected by structure-based alignment. The secondary structure elements and residue numbers from p40<sup>phox</sup> PB1 are shown above the sequences. The p67<sup>phox</sup> PB1 secondary structure elements shown below its sequence correspond to those of p40<sup>phox</sup> PB1 with the exception of α1', which is not present in p40<sup>phox</sup> PB1. The OPCA motif of p40<sup>phox</sup> PB1 is boxed in red. Residues for which C<sub>α</sub> coordinates superimpose are boxed with solid black lines. Residues with side chains forming inter-domain hydrogen bonds are shown with filled circles beneath them. Residues involved in intermolecular main chain hydrogen bonds are marked with filled squares. Basic cluster (BC) residues and the corresponding acidic cluster residues (AC) are highlighted in blue and red, respectively. Residues forming part of the BC but which are not involved in intermolecular hydrogen bonds are marked with open circles. Residues involved in intermolecular Van der Waals interactions are indicated by filled triangles. The C241V mutation in p40<sup>phox</sup> that was used for the crystallography is shown in lower case.

front of p40<sup>phox</sup> consisting of the β3/β4 loop, strand β4, and the N-terminal end of helix α2 (Figure 3C).

The p40<sup>phox</sup> surface contacting the p67<sup>phox</sup> PB1 has two clusters of acidic residues: acidic cluster one (AC1), consisting of Asp 289<sup>p40</sup>, Glu 291<sup>p40</sup>, and Asp 293<sup>p40</sup> in the β3/β4 loop; and AC2, consisting of Glu 301<sup>p40</sup> and Asp 302<sup>p40</sup> at the N-terminal end of helix α2 (Figure 3A). The importance of these acidic clusters for the interaction with the p67<sup>phox</sup> PB1 are supported by the observation that mutation of any of the AC1 or AC2 residues results in loss of binding (Nakamura et al., 1998). In cells stimulated by PMA or with a muscarinic receptor peptide, the D289A mutation results in a p40<sup>phox</sup> that is no longer able to stimulate NADPH oxidase activity (Kuribayashi et al., 2002). This mutant, in contrast to the wild-type, does not translocate to membranes upon cell stimulation and results in decreased membrane translocation of p47<sup>phox</sup> and p67<sup>phox</sup>. The residues analogous to the p40<sup>phox</sup> AC1 and AC2 are part of an acidic DX(D/E)GD-7(X)-(D/E)D sequence known as the OPCA motif that is present in many PB1 domains. The mutations S299F<sup>p40</sup> and D300K<sup>p40</sup> eliminate binding to the p67<sup>phox</sup> PB1 (Nakamura et al., 1998). These residues do not make direct intermolecular interactions in the heterodimer, but they may have a structural role in positioning the AC2-con-

taining helix α2 and the AC1-containing β3/β4 loop. Mutations of the analogous residues in cdc24 (S831A and D832A) do not eliminate binding to the Bem1p PB1 domain (Terasawa et al., 2001), further supporting that these residues do not directly mediate PB1 heterodimerization.

The p67<sup>phox</sup> surface contacting the p40<sup>phox</sup> PB1 has two prominent basic patches: basic cluster one (BC1), made up of Lys 355<sup>p67</sup> in strand β1 and Lys 418<sup>p67</sup> in the α2/β5 loop; and BC2, consisting of Lys 382<sup>p67</sup> at the C-terminal end of helix α1 and Lys365<sup>p67</sup> in strand β2 (Figure 3B).

The most striking features stabilizing the PB1/PB1 heterodimer are coulombic AC1/BC1 and AC2/BC2 interactions. In the DX(D/E)GD portion of AC1, the glycine residue has main chain torsional angles that would not be possible for a nonglycine residue and the presence of the glycine enables residues 291–293<sup>p40</sup> to form a tight hairpin with the side chains of Glu 291<sup>p40</sup> and Asp 293<sup>p40</sup> both directed toward Lys 355<sup>p67</sup> in BC1 (Figure 4). The observation that a K355A<sup>p67</sup> mutation eliminates heterodimerization and reduces NADPH oxidase activation in vivo points toward the essential role of this BC1 residue at the interface (Ito et al., 2001; Kuribayashi et al., 2002).

The human p40<sup>phox</sup>/p67<sup>phox</sup> PB1 heterodimer constitutes a very high-affinity interaction (K<sub>d</sub> = 4 nM [see

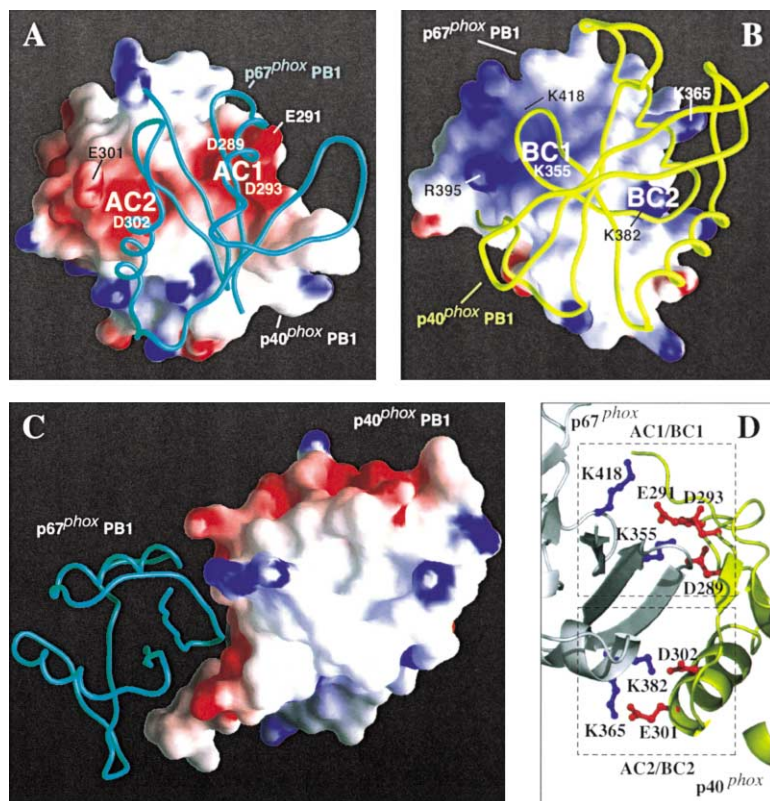


Figure 3. Surface Representations of the p40<sup>phox</sup> PB1/p67<sup>phox</sup> PB1 Heterodimer Showing the Distinct Electrostatic Complementarity of the Interface

(A) The “front” surface of p40<sup>phox</sup> PB1. The negative AC1 and AC2 patches on the “front” surface of p40<sup>phox</sup> PB1 interact with the positive BC1 and BC2, respectively, on the “back” of p67<sup>phox</sup> PB1. The surface of p40<sup>phox</sup> PB1 is colored by electrostatic potential (blue positive and red negative), and the p67<sup>phox</sup> PB1 is shown as a cyan-colored worm.

(B) The “back” surface of p67<sup>phox</sup> PB1 colored by electrostatic potential as in (A). The p40<sup>phox</sup> PB1 is shown as a yellow-colored worm.

(C) The p40<sup>phox</sup> PB1 has a concave “front” face into which the convex “back” face of p67<sup>phox</sup> PB1 fits. The representation is as in (A) with a view of the heterodimer rotated approximately 90° around the horizontal and vertical axes.

(D) The charged residues in the acidic and basic clusters at the p40<sup>phox</sup> PB1/p67<sup>phox</sup> PB1 interface are shown as balls and sticks. The view is rotated 180° about the horizontal axis relative to the view shown in (C).

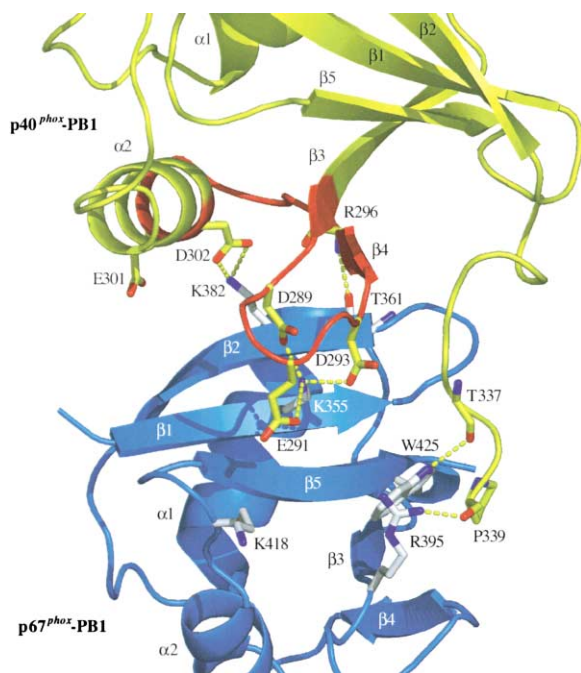


Figure 4. Details of the Interactions at the p40<sup>phox</sup> PB1/p67<sup>phox</sup> PB1 Heterodimer Interface

The domains are colored as in Figure 1. Dashed lines represent intermolecular hydrogen bonds. The side chains of residues involved in intermolecular hydrogen bonds or complementary electrostatic interactions as described in the text are shown as sticks.

Supplemental Figure S1 at <http://www.molecule.org/cgi/content/full/12/1/39/DC1> and 10 nM for the full-length proteins [Lapouge et al., 2002]) even though the total accessible surface area buried in the heterodimer interface is 1445 Å<sup>2</sup>, which is slightly less than the average value observed for crystal structures of dimeric proteins. Approximately 20% of this buried area is involved in the AC/BC interactions, while 45% is contributed by interactions between the p67<sup>phox</sup> PB1 and the C-terminal region of p40<sup>phox</sup> that is beyond the canonical PB1 domain as defined by the SMART database (residues 330–339). The importance of these p40<sup>phox</sup> C-terminal residues for the dimeric interaction is apparent from the observation that a construct lacking the p40<sup>phox</sup> C-terminal 5 residues does not bind p67<sup>phox</sup> (Nakamura et al., 1998). This C-terminal region forms an arm extending away from the surface of the p40<sup>phox</sup> PB1 and fitting onto the surface of the β1/β2 hairpin of the p67<sup>phox</sup> PB1. Several hydrophobic interactions in this portion of the interface as well as two hydrogen bonds (Arg 395<sup>p67</sup>–Pro339<sup>p40</sup> and Trp 425<sup>p67</sup>–Thr337<sup>p40</sup>, Figure 4) contribute to the stability of the heterodimer. Given the lack of sequence similarity in the C-terminal region among the proteins with PB1 domains, it is likely that this interaction not only contributes to stability but also to the specificity of PB1/PB1 heterodimerization observed in vivo and in vitro.

Interestingly, there is some sequence variation among NADPH oxidase PB1 domains from different species and between isotypes for the same species. Among the most striking of these sequence differences is seen in the homolog of p67<sup>phox</sup>, NOXA1 (p51), which associates

with the NOX1 isozyme (gp91<sup>phox</sup> homolog) of NADPH oxidase and which is expressed primarily in colon epithelium (Banfi et al., 2003; Geiszt et al., 2003). This homolog does not appear to have the basic residues in BC1 and BC2 characteristic of p67<sup>phox</sup>. Perhaps this sequence variation represents a mechanism to avoid cross-talk between NADPH oxidase isozymes. The sequence variation between species can manifest itself in different behaviors (Gauss et al., 2002). For example, the rabbit p67<sup>phox</sup> PB1 binds rabbit p40<sup>phox</sup> less efficiently than does human p67<sup>phox</sup> PB1 (see Supplemental Figure S2 at <http://www.molecule.org/cgi/content/full/12/1/39/DC1>). Given that animal models are often used to study phagocytosis and NADPH oxidase activation, the biological implication of these sequence variations across various species and isotypes warrants further investigation.

#### A CGD-Associated Mutation within the p67<sup>phox</sup> PB1 Domain

Most mutations associated with CGD involve the gp91<sup>phox</sup> or p47<sup>phox</sup> subunits of the NADPH oxidase (65% and 25%, respectively). The rest of CGD patients have mutations in p67<sup>phox</sup> or in p22<sup>phox</sup> (Cross et al., 2000; Heyworth et al., 2001). One point mutation, R395W, within the p67<sup>phox</sup> PB1 that affects NADPH oxidase activity, has been described in studies of CGD patients (Noack et al., 1999; Patiño et al., 1999). This mutation was reported in two patients with severe CGD who also had an in-frame deletion of residues 19–21 in the N-terminal TPR domain of p67<sup>phox</sup>, leading to an absence of p67<sup>phox</sup>. The recombinant p67<sup>phox</sup> R395W mutation resulted in NADPH oxidase that had only about 15% of the wild-type activity in a cell-free assay (Patiño et al., 1999). Our structure shows that Arg 395 makes a salt link with the C terminus of the p40<sup>phox</sup>. As a tryptophan, this salt link would not be possible and the mutation may also sterically hinder the interface. We find that the efficiency of heterodimerization between p67<sup>phox</sup> R395W PB1 and the p40<sup>phox</sup> PB1 is reduced about 50% compared to wild-type p67<sup>phox</sup> PB1 in GST pull-down assays (see Supplemental Figure S3 at <http://www.molecule.org/cgi/content/full/12/1/39/DC1>). The effect of this mutation emphasizes the importance of the p40<sup>phox</sup>/p67<sup>phox</sup> interactions through the PB1 domains for the function of NADPH oxidase in cells.

#### The Role of the PB1 Heterodimer in the Activation of NADPH Oxidase

The PB1 heterodimer links the p40<sup>phox</sup> subunit to the p67<sup>phox</sup> subunit, yet the role of p40<sup>phox</sup> for NADPH oxidase was not clear until recently when it was demonstrated that p40<sup>phox</sup> is capable of activating NADPH oxidase in stably transfected cells (Kuribayashi et al., 2002). p40<sup>phox</sup> is a potent stimulator (20-fold) of NADPH oxidase in response to a muscarinic receptor peptide that acts via a G<sub>i</sub>-dependent signaling, compared to a modest (2- to 3-fold) stimulation in response to PMA. This suggests that the contribution of p40<sup>phox</sup> to NADPH oxidase activation in vivo could be dependent on the specific stimulus and subsequent signaling pathway. Several mechanisms can be suggested for the molecular basis of p40<sup>phox</sup> stimulation of NADPH oxidase. First, it has been

shown that the PB1 domain-mediated heterodimerization is necessary for recruiting the cytosolic regulatory complex to the membrane fraction containing the NADPH oxidase. In this context, it may be relevant that p40<sup>phox</sup> has an N-terminal PX domain that mediates interactions with PtdIns3P-containing membranes, and phosphoinositides appear to be important activators of NADPH oxidase (Ellson et al., 2001; Brown et al., 2003; Peng et al., 2003). The p40<sup>phox</sup> subunit may also have a role as a chaperone that leads to mutual stabilization of p40<sup>phox</sup> and p67<sup>phox</sup> as suggested by the low levels of p40<sup>phox</sup> in CGD patients lacking p67<sup>phox</sup> (Wientjes et al., 1993; Tsunawaki et al., 1994).

#### Three Broad Classes of PB1 Domains

Because the folds of the PB1 domains from p40<sup>phox</sup> and p67<sup>phox</sup> are closely superimposable, it is reasonable to ask if these domains can homodimerize as well as heterodimerize. Gel filtration of both the isolated p40<sup>phox</sup> PB1 and p67<sup>phox</sup> PB1 domains show only a minor population of homodimers (data not shown), consistent with solution studies of the full-length proteins indicating them to be monomeric (Bravo et al., 2001; Grizot et al., 2001b; Lapouge et al., 2002). Superimposing the PB1 domains of p40<sup>phox</sup> and p67<sup>phox</sup> shows that the surfaces involved in intermolecular interactions in the heterodimer are distinct. The p67<sup>phox</sup> PB1 has a front surface that is structurally analogous to the front of p40<sup>phox</sup> (Figure 2B) but without the specific acidic residues necessary for interaction with another PB1 domain, including the acidic hairpin 291-EGD-293<sup>p40</sup>. Similarly, the “back” of p40<sup>phox</sup> is structurally analogous to the BC-containing “back” surface of p67<sup>phox</sup>, but it lacks a BC2.

Examining the sequences of all PB1 domains suggests that most of them can be classified into A-type PB1 domains that have a canonical OPCA motif, like cdc24 and p40<sup>phox</sup>, and B-type PB1 domains that have a signature of basic residues and lack the OPCA motif, like Bem1p and p67<sup>phox</sup> (Figure 2C). The distinct characters of these two types of PB1 domains means they tend to form heterodimers rather than an array of alternating front-to-back PB1 domains. Although A-type PB1 domains interact with B-type PB1 domains, there are interactions beyond the AC and BC clusters, such as the interaction of the p40<sup>phox</sup> C terminus with p67<sup>phox</sup> as revealed by our crystal structure, that are not conserved among the PB1 domains. It is probably these nonconserved interactions that give rise to the high specificity of PB1 heterodimerization that has been reported (Ito et al., 2001). The B-type p67<sup>phox</sup> PB1 does not interact with the A-type PB1 domain from cdc24 or with the PB1 domain from p62, and the A-type PB1 domain from p40<sup>phox</sup> does not interact with the B-type PB1 domain from Bem1p (Ito et al., 2001).

A small subset of PB1 domains has sequence motifs characteristic of both A-type and B-type domains, and we will refer to these as the AB-type domains. Among the AB-type domains are the PB1 domains of atypical protein kinase C isozymes (PKC $\lambda/\zeta$  and PKC $\xi$ ) and their adaptor proteins p62 and Par6. The aPKC isozymes are involved in a variety of signal transduction pathways, with the role of the aPKC dictated by interactions formed between its PB1 domain and the PB1 domains of its

adaptor proteins (Moscat and Diaz-Meco, 2000). Through its interaction with p62, aPKCs are recruited to activate the NF $\kappa$ B signaling pathway both in mammalian cells and in *Drosophila* (Sanz et al., 1999; Avila et al., 2002; Moscat et al., 2003). P62 also recruits PKC $\zeta$  to the Kv $\beta$ 2 subunit of the K $^{+}$  channel (Gong et al., 1999). Recent studies have established the importance of the interaction of PKC $\zeta$  with Par6 for cell polarity in several different contexts (Huynh et al., 2001; Ohno, 2001; Petronczki and Knoblich, 2001; Yamanaka et al., 2001; Gao et al., 2002; Etienne-Manneville and Hall, 2003b). PKC $\zeta$ , Par6, and p62 were previously noted as having an OPCA motif that could function as acidic clusters in the heterodimer interface. Interestingly, PKC $\zeta$  and Par6 also have critical residues that could function as basic clusters in the interface (Figure 2C). Based on the sequence alignment from the SMART database (Schultz et al., 2000), the p62 PB1 domain would not be expected to have key critical residues necessary for a functional B-type interface. However, a manual realignment of the p62 sequence, which included 12 additional N-terminal residues as shown in Figure 2C, indicates that p62, similarly to PKC $\zeta$  and Par6, has a B-type face in addition to the OPCA motif.

#### Par6 and p62 Do Not Use Their OPCA Motif to Interact with PKC $\zeta$

In order to resolve which interfaces p62, Par6, and PKC $\zeta$  actually use in formation of heterodimeric complexes, we constructed site-specific mutants of these proteins. Using GST pull-down binding assays, we find that PKC $\zeta$  interacts with both Par6 and p62 only when it has a wild-type OPCA motif on its front. Mutation D62A/D66A in the OPCA motif of PKC $\zeta$  abolishes binding to both Par6 and p62 PB1 domains (Figure 5A). The same mutation affects PKC $\zeta$  function in vivo (Gao et al., 2002). In contrast, a point mutation of a basic residue in the PKC $\zeta$  “back” (equivalent to Lys 355<sup>pb7</sup>) has no influence on binding to wild-type PB1 domains from p62 and Par6. This suggests that PKC $\zeta$  uses its acidic front to interact with the basic back of Par6 and p62. Consistent with this notion, mutation of a single basic residue at the back of either Par6 or p62 PB1 domains eliminates interaction with wild-type PKC $\zeta$ , whereas mutations of the acidic cluster at the front of these adaptors have no impact on binding to PKC $\zeta$  (Figure 5A). These results suggest that binding of the adaptor proteins p62 and Par6 to PKC $\zeta$  is mutually exclusive. Indeed, this is confirmed in direct competition experiments (see Supplemental Figure S4 at <http://www.molecule.org/cgi/content/full/12/1/39/DC1>).

#### P62 PB1 Domain Forms Front-To-Back Arrays

Gel filtration of p62-MBP fusions showed that most of the wild-type construct, as opposed to the mutants, is in high molecular weight aggregates in vitro (see Supplemental Figure S5 at <http://www.molecule.org/cgi/content/full/12/1/39/DC1>). This led us to question whether this domain, which has both OPCA and basic sequence motifs, might be capable of forming homotypic arrays using these motifs. When we performed GST pull-down assays using a p62-GST fusion with a mutated OPCA motif, we found that it efficiently cap-

tured either a wild-type p62-MBP or a K7A p62-MBP mutant (Figure 5B). In either of these cases, the basic back of the p62-GST binds to the OPCA motif of the p62-MBP. However, a p62-GST with a mutated OPCA motif cannot capture a p62-MBP with the same mutation, showing that a complex is formed only when there is one functional acidic face and one functional basic face between a pair of domains. These results show that the p62 PB1 domain forms homotypic front-to-back interactions. This conclusion is also supported by the observation that the mutant proteins do not show aggregation in gel filtration (see Supplemental Figure S5 at <http://www.molecule.org/cgi/content/full/12/1/39/DC1>). Our observations are consistent with yeast two-hybrid studies indicating that the PB1 domain from p62 is capable of interacting with itself (Puls et al., 1997; Gong et al., 1999). Given the front-to-back arrangement, there is no reason that p62 could not form large arrays (Figure 5C). P62 has been shown to form electron dense, punctate aggregates known as “sequestosomes” that include polyubiquitinated proteins (Shin, 1998). Both its ability to form self-arrays and its ability to interact with ubiquitinated proteins via a C-terminal ubiquitin-associated (UBA) domain (Figure 1A) may be important for the formation of punctate p62-containing “Mallory bodies” that have been observed associated with pathological damage to hepatocytes (Stumptner et al., 2002).

#### Structural Similarity to Other PB1 Domains

Our results showing the structural similarity of the PB1 domains from p40<sup>phox</sup> and p67<sup>phox</sup> are entirely consistent with sequence analysis suggesting that PC and PB1 domains are examples of the same type of domain. The PB1 domain of p67<sup>phox</sup> has a fold that resembles the PB1 domain from Bem1p, which was determined by NMR (Terasawa et al., 2001) (Figure 6A). However, the same NMR study suggested that the topology of the PB1 domain of the Bem1p binding partner, cdc24 (previously referred to as a PC domain) is very different from the p40<sup>phox</sup> PB1. The strand order that was reported for the cdc24 PB1 domain is 1-4-2-3 with all strands antiparallel (Figure 6B). The topology switch between cdc24 and p40<sup>phox</sup> PB1 domains can be visualized by starting from the p40<sup>phox</sup> topology and omitting strand  $\beta$ 1. This change of topology is surprising given that the PB1 domain from cdc24 contains the same conserved sequence features as p40<sup>phox</sup> and that it forms heterodimers with the Bem1 PB1 domain using these conserved residues. The cdc24 construct that was used in the NMR study consisted of residues 775–854, thereby lacking residues 761–774 of the consensus PB1 domain, a region analogous to strand  $\beta$ 1 of the p40<sup>phox</sup> PB1. It is possible that a construct starting with what is  $\beta$ 2 in p40<sup>phox</sup> would rearrange its hydrogen-bonding pattern so that  $\beta$ 2: $\beta$ 5 interactions would replace the  $\beta$ 1: $\beta$ 5 interactions that we see in the p40<sup>phox</sup> PB1.

#### Structural Similarity to the CAD Domains and Ras Binding Domains

The heterodimer formed from the regulatory domain of the caspase-activated DNase (CAD) and the inhibitor of CAD (iCAD) (Otomo et al., 2000) is similar to the PB1/PB1 heterodimer, and features of the CAD/iCAD interface

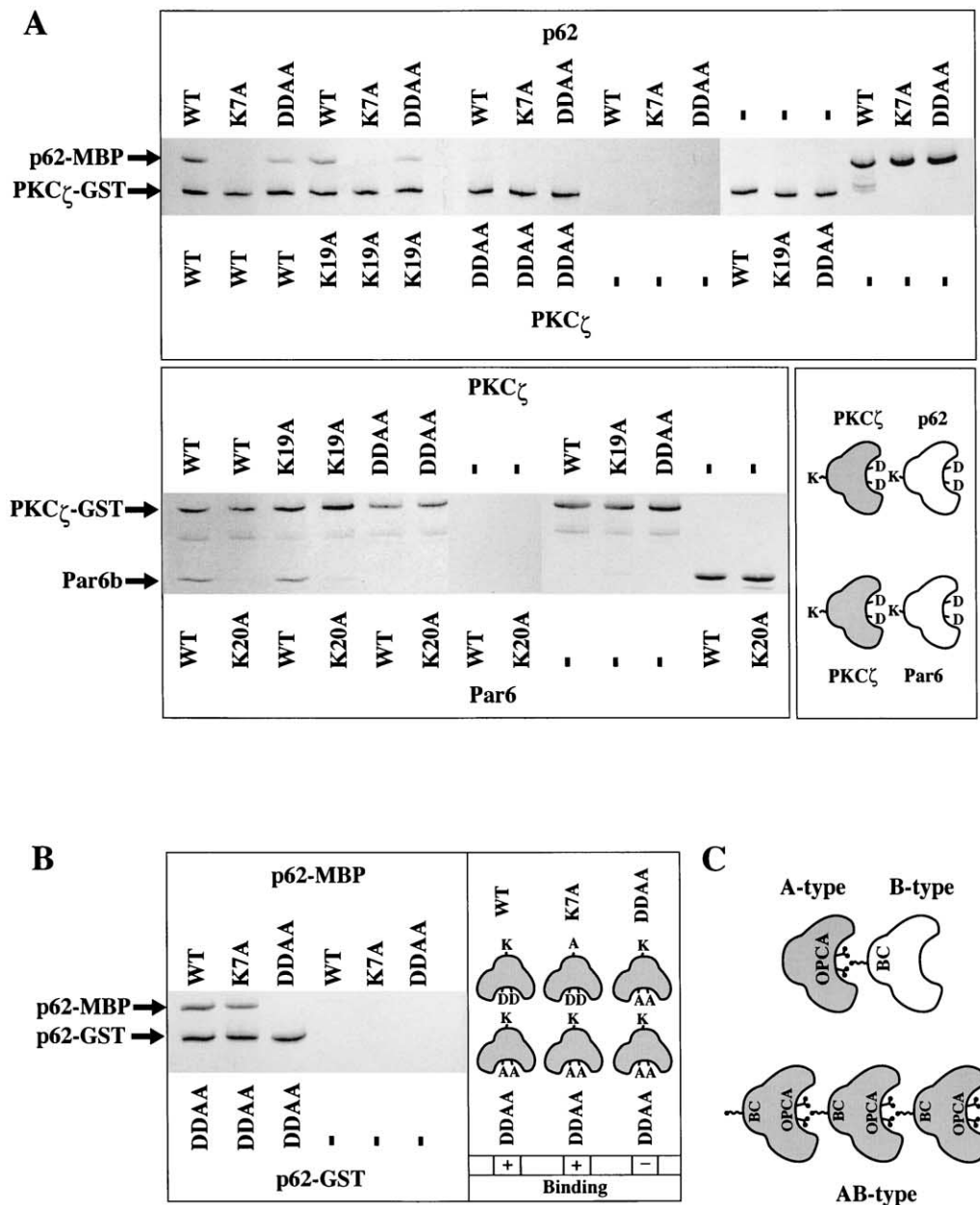
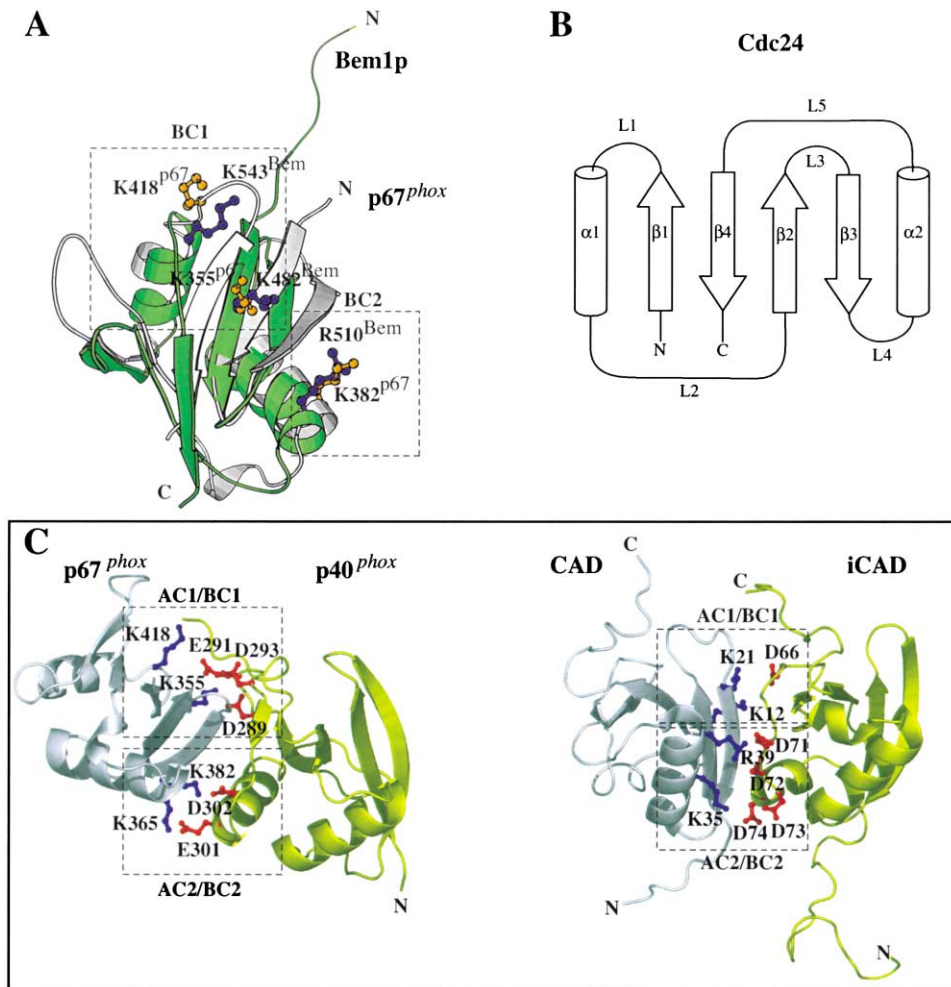


Figure 5. The Effect of Mutations in the PB1 Domains of PKC $\zeta$ , Par6, and p62 on Dimer Formation

(A) Effect of mutations in the OPCA and BC motifs on the formation of heterodimers between PKC $\zeta$ -GST and either p62-MBP (upper panel) or His<sub>6</sub>-Par6b (lower panel). Protein pairs were mixed in solution, incubated with glutathione resin, and bound material was eluted and separated by SDS PAGE. The lanes labeled DDAA correspond to mutants with two Asp to Ala mutations in the conserved OPCA motif (D62A and D66A for PKC $\zeta$ ; and D69A and D73A for p62). The lanes labeled with Lys to Ala mutations correspond to single-site mutations in the residue analogous to Lys 355<sup>67</sup> (present in BC1). The last six lanes at the right end of the upper panel and the last five lanes at the right end of the lower panel are PAGE analysis of samples of the purified proteins used in the GST pull-down assays. In the upper panel, p62 binds to PKC $\zeta$  only when the OPCA motif of PKC $\zeta$  is not mutated and the back of p62 has the wild-type Lys 7. The analogous result for PKC $\zeta$  interaction with Par6 in the lower panel shows that, similarly to p62, Par6b binds to PKC $\zeta$  only when the PKC $\zeta$  OPCA motif is not mutated and the back of Par6b has the wild-type Lys 20. The results, summarized in the lower right panel, show that the basic back of either p62 or Par6, but not their acidic OPCA motif, binds to the OPCA motif of PKC $\zeta$ . Because of the tendency of the wild-type p62 PB1 to form homooligomers, the amount of the wild-type p62 pulled down should not be compared quantitatively with that of the mutants.

(B) The effect of mutations in p62 PB1 on the formation of homodimers (left panel). The experiment was performed as in (A) except binding was between p62-MBP and p62-GST. The p62 PB1 can interact with itself as long as there is one partner with a wild-type OPCA motif on the front and one partner with a wild-type, basic back (right panel).

(C) A schematic diagram of the key front-to-back interactions in heterodimers involving one A-type and one B-type domain versus arrays of front-to-back AB-type PB1 domains.



**Figure 6.** Comparison of the p67<sup>phox</sup>/p40<sup>phox</sup> Heterodimer with the Bem1p/cdc24 and CAD/iCAD Heterodimers  
(A) Superposition of yeast Bem1p PB1 (green) and p67<sup>phox</sup> PB1 (rmsd 1.7 Å). The Bem1p residues K482, R510, and K543 are shown in blue with equivalent residues in p67<sup>phox</sup>, K355<sup>p67</sup>, K382<sup>p67</sup>, and K418<sup>p67</sup> colored in orange. The region in Bem1p that superimposes closely with  $\beta 4$  of p67<sup>phox</sup> PB1 has been shown as a  $\beta$  strand (although the region was not assigned as a  $\beta$  strand in the NMR study [Terasawa et al., 2001]). (B) Topology diagram of yeast Cdc24 PB1 domain as reported previously (Terasawa et al., 2001). (C) Comparison of acidic (red) and basic (blue) clusters at the p40<sup>phox</sup>/p67<sup>phox</sup> PB1 heterodimer interface with those at the interface of CAD/iCAD. The rmsd for superposition of p40<sup>phox</sup> on iCAD is 1.7 Å and the rmsd for superposition of p67<sup>phox</sup> on CAD is 2.1 Å.

suggest that these domains are probably homologous with the PB1 domains. The back of p67<sup>phox</sup> PB1, which is involved in the interface with p40<sup>phox</sup>, is analogous to the basic surface of CAD that interacts with an acidic surface of iCAD. In the CAD/iCAD heterodimer, there are two basic clusters on CAD (BC1 residues Lys 12 and Lys 21 and BC2 residues Lys 35 and Arg 39) that interact with two acidic clusters on iCAD (AC1 residue Asp 66 and AC2 residues Asp 71, Asp 72, Asp 73, and Asp 74). These AC1/BC1 and AC2/BC2 charge-charge interactions are analogous to those formed in the p40<sup>phox</sup>/p67<sup>phox</sup> heterodimer (Figure 6C). On the basis of their structural similarity and the similarity of key interacting residues in the heterodimer, the CAD/iCAD and PB1 domains were classified in the same SCOP superfamily (Lo Conte et al., 2002).

The  $\beta$  grasp fold present in PB1 domains is also present in the Ras binding domains (RBD) from RalGDS (Huang et al., 1998), Raf (Nassar et al., 1995), and phos-

phoinositide 3-kinase (Pacold et al., 2000). The RBDs and the PB1 domains are closely superimposable (Terasawa et al., 2001). Ras interacts with a surface of the RBD analogous to the basic surface of the p67<sup>phox</sup> PB1 domain that binds p40<sup>phox</sup>. However, the protein-protein interactions within the p40<sup>phox</sup>/p67<sup>phox</sup> PB1 heterodimers do not resemble those seen for the Ras/RBD heterodimers, and neither Bem1p nor p67<sup>phox</sup> PB1 domains bind Ras or Rap1a (Terasawa et al., 2001).

### Conclusion

The structure of the p40<sup>phox</sup> PB1/p67<sup>phox</sup> PB1 heterodimer shows the role of the OPCA motif in interdomain interactions. However, it also shows that additional interactions in the C-terminal tail of p40<sup>phox</sup> contribute to the affinity and specificity of the dimerization. A point mutation in p67<sup>phox</sup> PB1 associated with CGD maps to a region directly interacting with this C-terminal tail of p40<sup>phox</sup>. Surprisingly, our study of the interaction of p62 and Par6

Table 1. Data Collection, Structure Determination, and Refinement Statistics

Data Collection and MAD Phasing Statistics							
Data Set	Resolution (Å)	Observations/ Unique Reflections	Completeness (Last Shell)%	R <sub>merge</sub> <sup>a</sup>	<I/σ> (Last Shell)	Phasing Power (iso) <sup>b</sup>	Phasing Power (anom) <sup>b</sup>
Peak <sup>c</sup>	2.8	172391/22161	99.7 (100)	0.138	12.7 (5.6)	0.83	1.6
Inflection <sup>c</sup>	2.3	278018/39713	99.6 (99.2)	0.114	11.5 (2.6)	–	1.2
Remote <sup>c</sup>	2.0	357868/59062	97.7 (94.0)	0.155	8.7 (1.4)	0.98	1.1
TMLA <sup>f</sup>	2.4	202151/34796	97.3 (83.4)	0.122	11.1 (1.1)	1.0	0.89
Refinement Statistics							
Resolution (Å)	Protein Atoms	Waters	R <sub>cryst</sub> <sup>d</sup>	R <sub>free</sub> <sup>d</sup> (Data Used)%	Rmsd from Ideality <sup>e</sup>		
					Bonds	Angles	Dihedrals
129–2.0	6033	344	0.21	0.25 (5.0)	0.014 Å	1.4°	6.2°

Overall figure of merit 0.35 before solvent flattening and 0.80 after solvent flattening.

<sup>a</sup>  $R_{\text{merge}} = \sum_{hkl} \sum_i |I_i(hkl) - \langle I(hkl) \rangle| / \sum_{hkl} \sum_i I_i(hkl)$ .

<sup>b</sup> The phasing power is defined as the ratio of the rms value of the heavy atom structure factor amplitudes to the rms value of the lack-of-closure error.

<sup>c</sup> Data sets were collected at ESRF beamline ID29 at 12.6629keV, 12.6610keV, and 12.7061keV for the peak, inflection, and remote data sets, respectively.

<sup>d</sup>  $R_{\text{cryst}}$  and  $R_{\text{free}} = \sum |F_{\text{obs}} - F_{\text{calc}}| / \sum F_{\text{obs}}$ ;  $R_{\text{free}}$  calculated with the percentage of the data shown in parentheses.

<sup>e</sup> Rmsds for bond angles and lengths in regard to Engh and Huber parameters.

<sup>f</sup> Trimethyl lead acetate derivative of the Se-methionine-substituted protein. Data were collected on a rotating anode.

with PKC $\zeta$  indicates that the OPCA motif may be present in proteins that do not use it for intermolecular interactions. Although it has been noted that the OPCA motif is present in both PKC $\zeta$  and Par6 (Moscat and Diaz-Meco, 2000), our results show that Par6 interacts with PKC $\zeta$  using its basic “back” face rather than the OPCA-containing “front” face. These results suggest that various PKC $\zeta$ -dependent signaling pathways could be individually manipulated by mutating the basic faces of adaptors with which the PKC $\zeta$  PB1 domain interacts.

The example of p62 shows that a single PB1 domain can use both its front and back faces to make an array of front-to-back interacting PB1 domains, with a free end to which PKC $\zeta$  can be recruited. The ability of the p62-PB1 domain to form arrays may be relevant for the formation of pathological cellular p62-containing inclusions such as Mallory bodies and Lewy bodies (Zatloukal et al., 2002).

Although many PB1/PB1 domain interactions that have been examined are specific, this is not universally true. PKC $\zeta$  can use its acidic face to interact with either Par6 or p62. P62 can use its basic face to interact with either itself or with PKC $\zeta$ . There may be examples in which a single PB1 domain interacts simultaneously with two different PB1 domains, forming a heterotrimer. The structure of the PB1/PB1 heterodimer presented here will provide a useful framework for homology modeling that might provide clues as to what may be plausible binding partners for the whole family of PB1 domains.

## Experimental Procedures

### Protein Production

The sequences encoding residues 237–339 of p40<sup>phox</sup> and 352–429 of p67<sup>phox</sup> were cloned in vector pOPTG and expressed with a cleavable N-terminal GST tag. The p40<sup>phox</sup> PB1 domain has an engineered C242V mutation to prevent potential aggregation problems. Proteins were expressed in C41(DE3) cells grown at 37°C to an OD<sub>600nm</sub> = 1.0, then induced with 0.3 mM IPTG and incubated at 17°C for

12 hr. Se-Met-substituted proteins were grown in the methionine auxotroph B834(DE3) in M9 media supplemented with amino acids, seleno-(D,L)-methionine, and vitamins as described previously (Karthanassis et al., 2002). Cells were resuspended in buffer A (50 mM Tris, pH 7.5 [4°C], 1 mM EGTA, 1 mM EDTA, and 5 mM DTT) and disrupted with a French press. After ultracentrifugation, the supernatant was incubated with Glutathione Sepharose (Amersham, Uppsala, Sweden) for 1 hr at 4°C. The resin was washed with buffer A and then buffer B (50 mM Tris, pH 7.5, 200 mM NaCl, and 5 mM DTT). Tobacco etch virus protease (TEV) was then added at a mass ratio of 1:80 (TEV:PB1) and the resin was incubated at 4°C. After cleavage by TEV, the PB1 domain from p40<sup>phox</sup> retained an N-terminal GSHM linker sequence and p67<sup>phox</sup> retained an N-terminal GSHMA linker sequence. The individual PB1 domains were concentrated and purified by gel filtration on Superdex 75 16/60 equilibrated in buffer C (20 mM Tris, pH 7.4, 100 mM NaCl, and 5 mM DTT). The p40<sup>phox</sup> PB1 and a slight molar excess of p67<sup>phox</sup> PB1 were then mixed, and the complex was separated from excess monomer by gel filtration. The complex was concentrated to 9 mg/ml for crystallization screens.

The sequence encoding human p62 PB1 (residues 1–122) was generated by polymerase chain reaction (PCR) from the IMAGE clone 2906264 and cloned into pMAL-C2 vector (NEB, Beverly, MA) for expression as an MBP fusion. The cells were grown at 37°C to an optical density at OD<sub>600nm</sub> = 1.0, then induced with 0.3 mM IPTG at 37°C for 7 hr. The MBP fusion protein was purified on amylose resin (NEB). The protein was eluted with 10 mM maltose in PBS and further purified on Superdex S200 16/60. The majority of the wild-type protein eluted in the exclusion volume of the column. Two mutants of the p62 PB1 domain, K7A and DDAA, were also prepared by the same protocol.

The sequence encoding mouse Par6b PB1 (residues 1–129) was PCR amplified from IMAGE clone 2655658, cloned into pOPTG vector and expressed with an N-terminal MAH<sub>6</sub> tag. Par6b PB1 was expressed using the same growth conditions as for p40<sup>phox</sup> and purified with immobilized metal affinity chromatography and gel filtration on Superdex 75 16/60. The sequence encoding human PKC $\zeta$  PB1 (residues 1–130) was amplified from IMAGE clone 3835020, cloned in pOPTG, and expressed with an N-terminal GST tag using the same growth conditions as for p40<sup>phox</sup>. The PKC $\zeta$ -GST fusion was purified on glutathione sepharose resin followed by gel filtration on Superdex S200 16/60. The site-specific mutant K20A in the Par6b, K7A and D69A/D73A in the p62, and K19A and D62A/D66A in PKC $\zeta$  domain were created using overlapping PCR and

purified using the same procedures as for the wild-type. All the constructs were verified by sequencing.

#### In Vitro Binding Assays

Complex formation between PB1 domains was tested using GST pull-down assays. For the PKC $\zeta$ -GST/p62-MBP binding assays, 20  $\mu$ g (0.48 nmol) of PKC $\zeta$ -GST was incubated with 20  $\mu$ g (0.35 nmol) of p62-MBP in 500  $\mu$ l reactions containing PBS/0.5% Triton X-100 for 30 min on ice. For the PKC $\zeta$ -GST/Par6b binding assays, 55  $\mu$ g (1.3 nmol) of PKC $\zeta$ -GST was incubated with 24  $\mu$ g (1.5 nmol) of His6-Par6b. Control samples contained p62-MBP or His6-Par6b proteins without PKC $\zeta$ -GST. The samples were loaded in MicroSpin columns each containing 50  $\mu$ l bed volume Glutathione Sepharose beads (Amersham) equilibrated in PBS/0.5% Triton X-100, incubated for 45 min on a rotating wheel at 4°C, and then washed with 600  $\mu$ l PBS/0.5% Triton X-100 eight times. The columns were spun for 2 min at 3000 rpm, and the bound proteins were eluted with 50  $\mu$ l SDS sample buffer (for the PKC $\zeta$ -GST/p62-MBP binding assays) or with 10 mM glutathione in 50 mM Tris-HCl (pH 8.0) (for the PKC $\zeta$ -GST/Par6b binding assays) and run on 20% Phast SDS gels.

#### Crystallization and Heavy Atom Derivative

Solutions for 1200 crystallization conditions were dispensed into reservoirs of 96-well crystallization plates (Corning, Corning, NY). Protein (100 nl) and reservoir (100 nl) solutions were added to the plates as sitting drops using a Cartesian robot (Genomic Solutions, Huntingdon, UK). Final conditions were optimized in hanging drops by mixing 1  $\mu$ l of a 7.5 mg/ml solution of protein in buffer C with 1.2  $\mu$ l of a solution containing 18% PEG 3350, 17% PEG 400, 4.8% isopropanol, and 0.1 M CAPSO (pH 9.0). Drops were incubated at 17°C over a reservoir containing 18% PEG 3350, 17% PEG 400, and 0.1 M CAPSO (pH 9.0). For the trimethyl lead acetate (TMLA) derivative, a Se-Met-substituted crystal was soaked in a solution containing 5 mM TMLA for 5 min.

#### Data Collection, Phasing, and Model Refinement

Data were collected at 100 K. The TMLA derivative data set was collected with a rotating anode X-ray source and a MAR345 image plate. Multiple anomalous dispersion (MAD) data sets were collected at ESRF beamline ID29 using an ADSC CCD detector. Lead sites for the TMLA data set were located using the program SOLVE (Terwilliger and Berendzen, 1999) and refined with SHARP (de La Fortelle and Bricogne, 1997). Phases from the TMLA derivative were used with difference Fourier syntheses to locate the selenium sites for the MAD data sets. Maximum likelihood phases were refined with SHARP using the TMLA derivative and selenomethionine MAD data (Table 1). Solvent flattening was carried out with SOLOMON (Abrahams and Leslie, 1996) using a solvent content of 44.6% as optimized by SHARP. An initial model was built using Arp/warp (Perrakis et al., 1999) and refined by alternating rounds of refinement with REFMAC5 (CCP4, 1994) and manual rebuilding with the program O (Jones et al., 1991). Final statistics for the 2.0 Å model are given in Table 1. The PB1 heterodimer coordinates and structure factors have been deposited with the Protein Data Bank as entry 1OEY.

#### Acknowledgments

We thank Andrew McCarthy and Gordon Leonard for assistance with data collection at ESRF beamline ID29 and Elizabeth Duke for help at Daresbury SRS station 14.2. We thank Dmitry Veprintsev and Ralph Golbik for help with fluorescence spectroscopy and Phil Hawkins, Chris Ellison, Len Stephens, and Dirk Roos for helpful discussions. This work was supported by a grant from the British Heart Foundation (to R.L.W.) and a National Institutes of Health grant AR42426 (to M.T.Q.).

Received: January 28, 2003

Revised: May 2, 2003

Accepted: May 2, 2003

Published: July 24, 2003

#### References

- Abrahams, J.P., and Leslie, A.G.W. (1996). Methods used in the structure determination of bovine mitochondrial F1 ATPase. *Acta Crystallogr. D* 52, 30–42.
- Avila, A., Silverman, N., Diaz-Meco, M.T., and Moscat, J. (2002). The Drosophila atypical protein kinase C-ref(2)p complex constitutes a conserved module for signaling in the toll pathway. *Mol. Cell. Biol.* 22, 8787–8795.
- Babior, B.M. (1999). NADPH oxidase: an update. *Blood* 93, 1464–1476.
- Banfi, B., Clark, R.A., Steger, K., and Krause, K.H. (2003). Two novel proteins activate superoxide generation by the NADPH oxidase NOX1. *J. Biol. Chem.* 278, 3510–3513.
- Bateman, A., Birney, E., Durbin, R., Eddy, S.R., Howe, K.L., and Sonnhammer, E.L.L. (2000). The Pfam protein families data base. *Nucleic Acids Res.* 28, 263–266.
- Bravo, J., Karathanassis, D., Pacold, C.M., Pacold, M.E., Ellison, C.D., Anderson, K.E., Butler, P.J., Lavenir, I., Perisic, O., Hawkins, P.T., et al. (2001). The crystal structure of the PX domain from p40<sup>phox</sup> bound to phosphatidylinositol 3-phosphate. *Mol. Cell* 8, 829–839.
- Brown, G.E., Stewart, M.Q., Liu, H., Hal, V.-L., and Yaffe, M.B. (2003). A novel assay system implicates PtdIns(3,4)P<sub>2</sub>, PtdIns(3)P, and PKC $\delta$  in intracellular production of reactive oxygen species by the NADPH oxidase. *Mol. Cell* 11, 35–47.
- CCP4 (Collaborative Computing Project 4) (1994). The CCP4 suite: programs for protein crystallography. *Acta Crystallogr D* 50, 760–763.
- Croci, C., Brandstatter, J.H., and Enz, R. (2003). ZIP3, a new splice variant of the PKC- $\zeta$ -interacting protein family, binds to GABA<sub>A</sub> receptors, PKC- $\zeta$ , and Kv $\beta$ 2. *J. Biol. Chem.* 278, 6128–6135.
- Cross, A.R., Noack, D., Rae, J., Curnutte, J.T., and Heyworth, P.G. (2000). Hematologically important mutations: the autosomal recessive forms of chronic granulomatous disease (first update). *Blood Cells Mol. Dis.* 26, 561–565.
- de La Fortelle, E., and Bricogne, G. (1997). Maximum-likelihood heavy-atom parameter refinement for multiple isomorphous replacement and multiwavelength anomalous diffraction methods. *Methods Enzymol.* 276, 472–494.
- Ellison, C.D., Gobert-Gosse, S., Anderson, K.E., Davidson, K., Erdjument-Bromage, H., Tempst, P., Thuring, J.W., Cooper, M.A., Lim, Z.-Y., Holmes, A.B., et al. (2001). PtdIns(3)P regulates the neutrophil oxidase complex by binding to the PX domain of p40<sup>phox</sup>. *Nat. Cell Biol.* 3, 679–682.
- Etienne-Manneville, S., and Hall, A. (2003a). Cdc42 regulates GSK-3 $\beta$  and adenomatous polyposis coli to control cell polarity. *Nature* 421, 753–756.
- Etienne-Manneville, S., and Hall, A. (2003b). Cell polarity: Par6, aPKC and cytoskeletal crosstalk. *Curr. Opin. Cell Biol.* 15, 67–72.
- Gao, L., Joberty, G., and Macara, I.G. (2002). Assembly of epithelial tight junctions is negatively regulated by Par6. *Curr. Biol.* 12, 221–225.
- Gauss, K.A., Mascolo, P.L., Siemsen, D.W., Nelson, L.K., Bunger, P.L., Pagano, P.J., and Quinn, M.T. (2002). Cloning and sequencing of rabbit leukocyte NADPH oxidase genes reveals a unique p67<sup>phox</sup> homolog. *J. Leukoc. Biol.* 71, 319–328.
- Geiszt, M., Lekstrom, K., Witta, J., and Leto, T.L. (2003). Proteins homologous to p47<sup>phox</sup> and p67<sup>phox</sup> support superoxide production by NAD(P)H oxidase 1 in colon epithelial cells. *J. Biol. Chem.* 278, 20006–20012.
- Gong, J., Xu, J., Bezanilla, M., van Huizen, R., Derin, R., and Li, M. (1999). Differential stimulation of PKC phosphorylation of potassium channels by ZIP1 and ZIP2. *Science* 285, 1565–1569.
- Grizot, S., Fieschi, F., Dagher, M.-C., and Pebay-Peyroula, E. (2001a). The active N-terminal region of p67<sup>phox</sup>. Structure at 1.8 Å resolution and biochemical characterizations of the A128V mutant implicated in chronic granulomatous disease. *J. Biol. Chem.* 276, 21627–21631.
- Grizot, S., Grandvaux, N., Fieschi, F., Fauré, J., Massenet, C., An-

- drieu, J.-P., Fuchs, A., Vignais, P.V., Timmins, P.A., Dagher, M.-C., et al. (2001b). Small angle neutron scattering and gel filtration analyses of neutrophil NADPH oxidase cytosolic factors highlight the role of the C-terminal end of p47<sup>phox</sup> in the association with p40<sup>phox</sup>. *Biochemistry* 40, 3127–3133.
- Heyworth, P.G., Curnutte, J.T., Rae, J., Noack, D., Roos, D., van Koppen, E., and Cross, A.R. (2001). Hematologically important mutations: X-linked chronic granulomatous disease (second update). *Blood Cells Mol. Dis.* 27, 16–26.
- Hiroaki, H., Ago, T., Ito, T., Sumimoto, H., and Kohda, D. (2001). Solution structure of the PX domain, a target of the SH3 domain. *Nat. Struct. Biol.* 8, 526–530.
- Huang, L., Hofer, F., Martin, G.S., and Kim, S.-H. (1998). Structural basis for the interaction of Ras with RalGDS. *Nat. Struct. Biol.* 5, 422–426.
- Huynh, J.R., Petronczki, M., Knoblich, J.A., and St Johnston, D. (2001). Bazooka and PAR-6 are required with PAR-1 for the maintenance of oocyte fate in *Drosophila*. *Curr. Biol.* 11, 901–906.
- Ito, T., Matsui, Y., Ago, T., Ota, K., and Sumimoto, H. (2001). Novel modular domain PB1 recognizes PC motif to mediate functional protein-protein interactions. *EMBO J.* 20, 3938–3946.
- Jones, T.A., Zou, J.-Y., Cowan, S.W., and Kjeldgaard, M. (1991). Improved methods for building protein models in electron density maps and the location of errors in these models. *Acta Crystallogr. A* 47, 110–119.
- Kami, K., Takeya, R., Sumimoto, H., and Kohda, D. (2002). Diverse recognition of non-PxxP peptide ligands by the SH3 domains from p67<sup>phox</sup>, Grb2 and Pex13p. *EMBO J.* 21, 4268–4276.
- Karathanassis, D., Stahelin, R.V., Bravo, J., Perisic, O., Pacold, C.M., Cho, W., and Williams, R.L. (2002). Binding of the PX domain of p47<sup>phox</sup> to phosphatidylinositol 3,4-bisphosphate and phosphatidic acid is masked by an intramolecular interaction. *EMBO J.* 21, 5057–5068.
- Kuribayashi, F., Nuno, H., Wakamatsu, K., Tsunawaki, S., Sato, K., Ito, T., and Sumimoto, H. (2002). The adaptor protein p40<sup>phox</sup> as a positive regulator of the superoxide-producing phagocyte oxidase. *EMBO J.* 21, 6312–6320.
- Lapouge, K., Smith, S.J.M., Walker, P.A., Gamblin, S.J., Smerdon, S.J., and Rittinger, K. (2000). Structure of the TPR domain of p67<sup>phox</sup> in complex with Rac•GTP. *Mol. Cell* 6, 899–907.
- Lapouge, K., Smith, S.J., Groemping, Y., and Rittinger, K. (2002). Architecture of the p40-p47-p67<sup>phox</sup> complex in the resting state of the NADPH oxidase: a central role for p67<sup>phox</sup>. *J. Biol. Chem.* 277, 10121–10128.
- Lo Conte, L., Brenner, S.E., Hubbard, T.J., Chothia, C., and Murzin, A.G. (2002). SCOP database in 2002: refinements accommodate structural genomics. *Nucleic Acids Res.* 30, 264–267.
- Moscat, J., and Diaz-Meco, M.T. (2000). The atypical protein kinase Cs. Functional specificity mediated by specific protein adapters. *EMBO Rep.* 1, 399–403.
- Moscat, J., Diaz-Meco, M.T., and Rennert, P. (2003). NF- $\kappa$ B activation by protein kinase C isoforms and B-cell function. *EMBO Rep.* 4, 31–36.
- Nakamura, R., Sumimoto, H., Mizuki, K., Hata, K., Ago, T., Kitajima, S., Takeshige, K., Sakaki, Y., and Ito, T. (1998). The PC motif: a novel and evolutionarily conserved sequence involved in interaction between p40<sup>phox</sup> and p67<sup>phox</sup>, SH3 domain-containing cytosolic factors of the phagocyte NADPH oxidase. *Eur. J. Biochem.* 251, 583–589.
- Nassar, M., Horn, G., Herrmann, C., Scherer, A., McCormick, F., and Wittinghofer, A. (1995). The 2.2 Å crystal structure of the Ras-binding domain of the serine/threonine kinase c-Raf1 in complex with Rap1A and a GTP analogue. *Nature* 375, 554–560.
- Noack, D., Rae, J., Cross, A.R., Munoz, J., Salmen, S., Mendoza, J.A., Rossi, N., Curnutte, J.T., and Heyworth, P.G. (1999). Autosomal recessive chronic granulomatous disease caused by novel mutations in NCF-2, the gene encoding the p67<sup>phox</sup> component of phagocyte NADPH oxidase. *Hum. Genet.* 105, 460–467.
- Ohno, S. (2001). Intercellular junctions and cellular polarity: the PAR-aPKC complex, a conserved core cassette playing fundamental roles in cell polarity. *Curr. Opin. Cell Biol.* 13, 641–648.
- Otomo, T., Sakahira, H., Uegaki, K., Nagata, S., and Yamazaki, T. (2000). Structure of the heterodimeric complex between CAD domains of CAD and ICAD. *Nat. Struct. Biol.* 7, 658–662.
- Pacold, M.E., Suire, S., Perisic, O., Lara-Gonzalez, S., Davis, C.T., Walker, E.H., Hawkins, P.T., Stephens, L., Eccleston, J.F., and Williams, R.L. (2000). Crystal structure and functional analysis of Ras binding to its effector phosphoinositide 3-kinase gamma. *Cell* 103, 931–943.
- Patiño, P.J., Rae, J., Noack, D., Erickson, R., Ding, J., de Olarte, D.G., and Curnutte, J.T. (1999). Molecular characterization of autosomal recessive chronic granulomatous disease caused by a defect of the NADPH oxidase component p67<sup>phox</sup>. *Blood* 94, 2505–2514.
- Peng, G., Huang, J., Boyd, M., and Kleinberg, M.E. (2003). Properties of phagocyte NADPH oxidase p47<sup>phox</sup> mutants with unmasked SH3 domains: full reconstitution of oxidase activity in a semi-recombinant cell-free system lacking arachidonic acid. *Biochem. J.* 373, 221–229.
- Perrakis, A., Morris, R., and Lamzin, V.S. (1999). Automated protein model building combined with iterative structure refinement. *Nat. Struct. Biol.* 6, 458–463.
- Petronczki, M., and Knoblich, J.A. (2001). DmPAR-6 directs epithelial polarity and asymmetric cell division of neuroblasts in *Drosophila*. *Nat. Cell Biol.* 3, 43–49.
- Plant, P.J., Fawcett, J.P., Lin, D.C., Holdorf, A.D., Binns, K., Kulkarni, S., and Pawson, T. (2003). A polarity complex of mPar-6 and atypical PKC binds, phosphorylates and regulates mammalian Lgl. *Nat. Cell Biol.* 5, 301–308.
- Ponting, C.P. (1996). Novel domains in NADPH oxidase subunits, sorting nexins, and PtdIns 3-kinases: binding partners of SH3 domains? *Protein Sci.* 5, 2353–2357.
- Ponting, C.P., Ito, T., Moscat, J., Diaz-Meco, M.T., Inagaki, F., and Sumimoto, H. (2002). OPR, PC and AID: all in the PB1 family. *Trends Biochem. Sci.* 27, 10.
- Puls, A., Schmidt, S., Grawe, F., and Stabel, S. (1997). Interaction of protein kinase C zeta with ZIP, a novel protein kinase C-binding protein. *Proc. Natl. Acad. Sci. USA* 94, 6191–6196.
- Roccatò, E., Pagliardini, S., Cleris, L., Canevari, S., Formelli, F., Pierotti, M.A., and Greco, A. (2003). Role of TFG sequences outside the coiled-coil domain in TRK-T3 oncogenic activation. *Oncogene* 22, 807–818.
- Sanz, L., Sanchez, P., Lallena, M.J., Diaz-Meco, M.T., and Moscat, J. (1999). The interaction of p62 with RIP links the atypical PKCs to NF- $\kappa$ B activation. *EMBO J.* 18, 3044–3053.
- Schultz, J., Copley, R.R., Doerks, T., Ponting, C.P., and Bork, P. (2000). SMART: a web-based tool for the study of genetically mobile domains. *Nucleic Acids Res.* 28, 231–234.
- Shin, J. (1998). P62 and the sequestosome, a novel mechanism for protein metabolism. *Arch. Pharm. Res.* 21, 629–633.
- Stumptner, C., Fuchsbichler, A., Heid, H., Zatloukal, K., and Denk, H. (2002). Mallory body—a disease-associated type of sequestosome. *Hepatology* 35, 1053–1062.
- Sun, W., Kesavan, K., Schaefer, B.C., Garrington, T.P., Ware, M., Johnson, N.L., Gelfand, E.W., and Johnson, G.L. (2001). MEKK2 associates with the adapter protein Lad/RIBP and regulates the MEK5-BMK1/ERK5 pathway. *J. Biol. Chem.* 276, 5093–5100.
- Terasawa, H., Noda, Y., Ito, T., Hatanaka, H., Ichikawa, S., Ogura, K., Sumimoto, H., and Inagaki, F. (2001). Structure and ligand recognition of the PB1 domain: a novel protein module binding to the PC motif. *EMBO J.* 20, 3947–3956.
- Terwilliger, T.C., and Berendzen, J. (1999). Automated structure solution for MIR and MAD. *Acta Crystallogr. D* 55, 849–861.
- Tsunawaki, S., Mizunari, H., Nagata, M., Tatsuzawa, O., and Kuratsui, T. (1994). A novel cytosolic component, p40<sup>phox</sup>, of respiratory burst oxidase associates with p67<sup>phox</sup> and is absent in patients with chronic granulomatous disease who lack p67<sup>phox</sup>. *Biochem. Biophys. Res. Commun.* 199, 1378–1387.

Wientjes, F.B., Hsuan, J.J., Totty, N.F., and Segal, A.W. (1993). p40<sup>phox</sup>, a third cytosolic component of the activation complex of the NADPH oxidase to contain src homology 3 domains. *Biochem. J.* 296, 557–561.

Yamanaka, T., Horikoshi, Y., Suzuki, A., Sugiyama, Y., Kitamura, K., Maniwa, R., Nagai, Y., Yamashita, A., Hirose, T., Ishikawa, H., et al. (2001). PAR-6 regulates aPKC activity in a novel way and mediates cell-cell contact-induced formation of the epithelial junctional complex. *Genes Cells* 6, 721–731.

Zatloukal, K., Stumptner, C., Fuchsbichler, A., Heid, H., Schnoelzer, M., Kenner, L., Kleinert, R., Prinz, M., Aguzzi, A., and Denk, H. (2002). p62 is a common component of cytoplasmic inclusions in protein aggregation diseases. *Am. J. Pathol.* 160, 255–263.

#### Accession Numbers

The PB1 heterodimer coordinates and structure factors have been deposited with the Protein Data Bank as entry 1OEY.